Resonant coupling between localized plasmons and anisotropic molecular coatings in ellipsoidal metal nanoparticles

Tobias Ambjörnsson*
NORDITA (Nordic Institute for Theoretical Physics), Blegdamsvej 17, DK-2100 Copenhagen Ø, Denmark

Gautam Mukhopadhyay
Physics Department, Indian Institute of Technology, Bombay, Powai, Mumbai 400076, India

S. Peter Apell and Mikael Käll
Department of Applied Physics, Chalmers University of Technology and Göteborg University, 412 96 Göteborg, Sweden
(Received 2 September 2005; revised manuscript received 6 January 2006; published 16 February 2006)

We present an analytic theory for the optical properties of ellipsoidal plasmonic particles covered by anisotropic molecular layers. The theory is applied to the case of a prolate spheroid covered by chromophores oriented parallel and perpendicular to the metal surface. For the case that the molecular layer resonance frequency is close to being degenerate with one of the particle plasmon resonances strong hybridization between the two resonances occurs. Approximate analytic expressions for the hybridized resonance frequencies, their extinction cross-section peak heights, and widths are derived. The strength of the molecular-plasmon interaction is found to be strongly dependent on molecular orientation and suggests that this sensitivity could be the basis for novel nanoparticle based bio- and chemo-sensing applications.

DOI: 10.1103/PhysRevB.73.085412 PACS number(s): 71.45.Gm, 33.70.Jg, 03.50.De

I. INTRODUCTION

The recent decade has witnessed extensive research efforts directed at localized surface plasmons (LSP's)—i.e., resonant charge-density oscillations confined to subwavelength metal structures, such as particles,[1] holes,[2] shells,[3] or rods.[4] LSP's are important because they lead to strongly enhanced optical absorption and scattering cross sections and because they readily couple to optical far fields, unlike the ordinary surface plasmons of extended metal surfaces. In the small-particle regime, the LSP resonance wavelengths of a single nanostructure are uniquely determined by its shape and dielectric function and by the optical constants of the embedding medium. Thus, the color of the nanostructure can be tuned over an extended wavelength range, including most of the visible and infrared regions in the case of silver or gold structures, through a variation in shape. Moreover, the color can be used to "sense" the optical properties of the surrounding. In addition, excitation of LSP's leads to strongly enhanced and localized fields in certain regions near the metal surface and these fields can be used to amplify various molecular cross sections. A bisphere system, for example, supports resonances for which the field is concentrated in the gap between the spheres, which is crucial for single-molecule surface-enhanced Raman scattering[5] (SERS), and a sharp point or protrusion support LSP-enhanced fields at its apex, which can be utilized for various types of near-field microscopy.[6] Sensing applications rely on the fact that it is only the optical properties of the material within the zone of high field enhancement that strongly affect the LSP resonance condition.[7] The LSP spectrum, which can be measured through far-field extinction or Rayleigh scattering spectroscopy, can therefore be used for ultrasensitive sensing applications aimed, for example, at quantifying various biomolecular recognition reactions.[8,9]

As is known from a range of experiments and calculations on nanostructured or flat metal surfaces covered with chromophores, such as dye molecules, the interaction between a plasmonic structure and its dielectric environment can be very strong if the dielectric possesses an optical resonance that is degenerate with a surface plasmon resonance mode.[10–17] This strong coupling also forms the basis for important applications in molecular spectroscopy, in particular surface-enhanced resonance Raman scattering (SERRS) and surface-enhanced fluorescence.[18–20] For atoms and molecules confined in microcavities similar strong coupling can occur.[21,22] In many applications, it is advantageous to bind the molecular layer to the metal via specific functional groups—for example, thiols—in which case the molecular transition dipole moment will have a more or less well-defined orientation relative to the local fields generated at plasmon resonance. This will in turn affect the degree of coupling between a molecular resonance and a plasmon.

In this work, we present an analytical theory for calculating the optical properties of a subwavelength metallic ellipsoid, the prototypical example of a nanostructure supporting tunable LSP's, covered by an optically anisotropic molecular layer. We then utilize this formalism for investigating strong coupling effects in nanoplasmonics. The quasistatic theory of dipolar plasmons for ellipsoids has played an important role in nano-optics, as it can be used to model a wide range of nanoparticle shapes of practical interest, including rods, spheres, and oblate and prolate particles, accessing a broad range of frequencies. The extension of this theory to ellipsoidal cores with anisotropic coatings means that it is now possible to also investigate the effect of molecular orientation relative to the core surface.

II. THEORY

While the polarizability of a metallic particle with and without coating has been studied in the past and can be found in textbooks, to our knowledge, the effect of anisotropy—i.e., molecular orientation—has not been analyzed earlier in the context of plasmonics. Here, we recapitulate recent analytic results[23,24] for the dipolar polarizability of an ellipsoid with an anisotropic coating [the coating dielectric function being different parallel and perpendicular to the coating normal; see Fig. 1(a)] and combine these results with realistic microscopic dielectric functions for the metallic nanoparticle and the coating.

The system we have in mind is depicted in Fig. 1(a): We consider a coated ellipsoidal particle in an external electric field $\vec{E}_0$, with field component $E_{0\upsilon}$ in the υ direction ($\upsilon=x,y,z$). The frequency of the external field is $\omega=2\pi c/\lambda$, where c is the speed of light and λ is the wavelength. The principal semiaxes of the inner and outer ellipsoids are a_υ and b_υ with $a_x \geqslant a_y \geqslant a_z$ and $b_x \geqslant b_y \geqslant b_z$. The shape of the coated particle is completely specified by the ellipticity of the inner surface, $e_i^2 \equiv 1-a_z^2/a_x^2$; the ellipticity of the outer surface, $e_o^2 \equiv 1-b_z^2/b_x^2$ ($e_i^2=e_o^2=0$ for a sphere); and $s \equiv (a_x^2-a_y^2)/(a_x^2-a_z^2)$; e_i^2, e_o^2, and s are all in the range [0,1]. The coating thickness is determined by the relative coating volume $\Delta_V=V_{\text{coat}}/V_o$, where $V_o=4\pi b_x b_y b_z/3$ is the total ellipsoidal volume and $V_{\text{coat}}=V_o-V_i$ is the coating volume ($V_i=4\pi a_x a_y a_z/3$ is the volume of the inner ellipsoid). For the case of a thin coating the ellipticities are related: $e_i^2=e_o^2(1+\bar{\delta})$, where $\bar{\delta}$ is the relative coating thickness parameter (see Refs. 23 and 24); the relative coating volume (a dimensionless entity) introduced above can be written in terms of the parameter $\bar{\delta}$ according to $\Delta_V=F_o\bar{\delta}/2$, where $F_o=1+(1-se_o^2)^{-1}+(1-e_o^2)^{-1}$ (see Ref. 24). The "material" properties of the coated nanoparticle enter through the relevant dielectric functions: We denote the dielectric function of the inner ellipsoid by $\varepsilon_{\text{in}}(\omega)$. The coating has dielectric function $\varepsilon_{c\|}(\omega)$ in the normal direction and $\varepsilon_{c\perp}(\omega)$ in the tangential direction. The dielectric function of the surrounding medium is assumed to be real and frequency independent and is denoted by ε_{m}. The entities above completely determine the electromagnetic response of a coated ellipsoidal particle—i.e., determine, for instance, the particle polarizability $\alpha_{\upsilon\upsilon}$ and the electric field distribution in and around the coated ellipsoid.[23,24]

The full expression for the dipolar polarizability $\alpha_{\upsilon\upsilon}$ (defined through $p_\upsilon=4\pi\varepsilon_0\varepsilon_m\alpha_{\upsilon\upsilon}E_{0\upsilon}$, where p_υ is the υ component, $\upsilon=x$, y, or z, of the induced dipole moment, and ε_0 is the permittivity of free space) in terms of the geometric and dielectric entities above is given in Refs. 23 and 24: Knowledge of $\alpha_{\upsilon\upsilon}$ requires a function $H_\upsilon(u,s;q)$, satisfying Heun's equation,[25,26] evaluated at the inner, $q=e_i^2$, and the outer, $q=e_o^2$, surfaces. The shape parameter s was introduced above. The anisotropy in the dielectric function of the coating ($\varepsilon_{c\|}$ and $\varepsilon_{c\perp}$) enters through u defined as

$$u = u_\pm = -\frac{1}{2} \pm \frac{1}{2}(1+8\varepsilon_\perp\varepsilon_\|^{-1})^{1/2}, \tag{1}$$

where $\varepsilon_\mu(\omega)=\varepsilon_{c\mu}(\omega)/\varepsilon_m$ ($\mu=\perp$ or $\|$). For the case of spheroids (two of the principal axes are equal) $H_\upsilon(u,s;q)$ is expressible in terms of hypergeometric functions, which are available in standard mathematical numerical packages, such as MatLab or Mathematica. For general ellipsoids $H_\upsilon(u,s;q)$ is straightforwardly generated using a recurrence relation, explicitly given in Ref. 23. Introducing a second function $r_\upsilon(u,s;q)$ ($\upsilon=x$, y, or z), required while implementing the

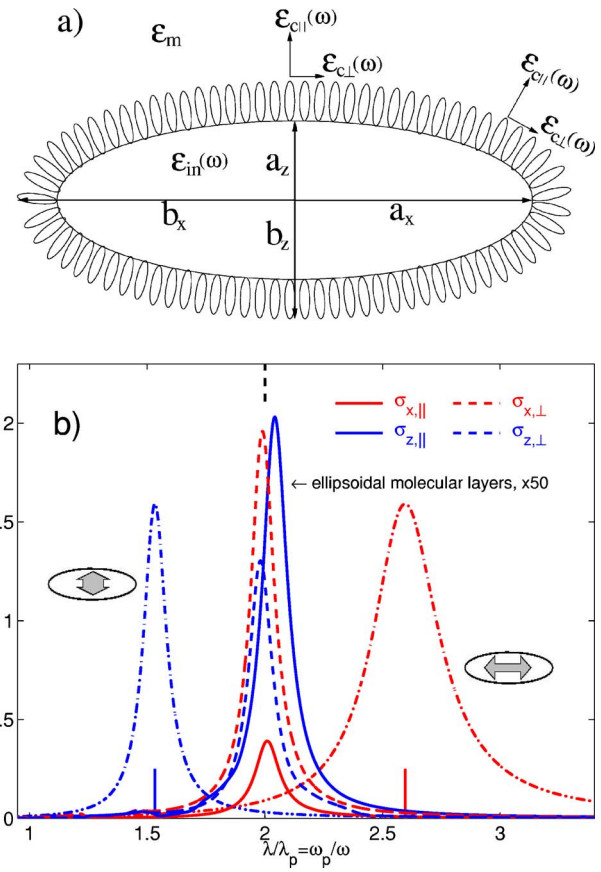

FIG. 1. (Color online) (a) A cut through a coated ellipsoidal nanoparticle. The principal semiaxes perpendicular to the paper are a_y and b_y, respectively. The relevant dielectric functions $\epsilon_{in}(\omega)$, $\varepsilon_{c\|}(\omega)$, $\varepsilon_{c\perp}(\omega)$, and ε_m are also indicated. (b) Extinction spectrum, where $\sigma_{\upsilon\upsilon}=\omega\,\text{Im}[\alpha_{\upsilon\upsilon}]$, $\upsilon=x,y,z$. The dash-dotted curves are for an *uncoated* metallic ellipsoid, where the red (blue) curve is for the external field along the x axis (z axis). The red solid (x direction) and blue solid (z direction) curves correspond to the case of an ellipsoidal molecular layer (*without* an interior metallic region; i.e., we set $\epsilon_i=1$) with a resonance *parallel* to the layer normal. Here, this situation is modeled by taking $\gamma_{0\|}/v_0=0.2$, $\gamma_{\infty\|}/v_0=0.02$, and $\gamma_{0\perp}/v_0=\gamma_{\infty\perp}/v_0=0.01$ (corresponding to effective oscillator strength $c_{0\|}\approx 2.26$ and large frequency refractive index $n_\|\approx 1.06$; see text). The red dashed (x direction) and blue dashed (z direction) curves are for the case that the molecular layer has a resonance *perpendicular* to the layer normal. We take $\gamma_{0\perp}/v_0=0.1$ and $\gamma_{\infty\perp}/v_0=\gamma_{0\|}/v_0=\gamma_{\infty\|}/v_0=0.01$ (so that $c_{0\perp}\approx 1.13$ and $n_\perp\approx 1.07$). The following parameters were used: $e_o^2=0.8$, $s=1$, $\Delta_V=0.08$, $\Gamma_p/\omega_p=0.05$, $\omega_{0\|}/\omega_p=\omega_{0\perp}/\omega_p=0.5$, $\Gamma_\|/\omega_p=\Gamma_\perp/\omega_p=0.03$, and $\varepsilon_m=1$. The extinction cross sections are shown in units of the total volume V_o. The solid and dashed vertical bars indicate the plasmon and molecular resonance frequencies, respectively. Notice the small peak heights of the molecular layer resonances (here enlarged by a factor of 50) compared with the plasmon resonance heights.

boundary conditions and defined in terms of $H_v(u,s;q)$ according to

$$r_v(u,s;q) = 1 - f_v(s;q)\left\{1 - u + 2q\frac{\partial}{\partial q}\ln[H_v(u,s;q)]\right\}, \tag{2}$$

where $f_x(s;q)=1$, $f_y(s;q)=1-sq$, and $f_z(s;q)=1-q$, the polarizability of an ellipsoid with an anisotropic coating is

$$\alpha_{vv} = \frac{V_o}{4\pi n_v^o}\frac{I_v(\kappa=-1)}{I_v(\kappa=1/n_v^o-1)}, \tag{3}$$

where

$$I_v(\kappa) = [r_v^o(u_+) + \kappa\varepsilon_\parallel^{-1}][r_v^i(u_-) - \varepsilon_i\varepsilon_\parallel^{-1}] - \rho_v[r_v^o(u_-) + \kappa\varepsilon_\parallel^{-1}] \times [r_v^i(u_+) - \varepsilon_i\varepsilon_\parallel^{-1}], \tag{4}$$

where $\varepsilon_i=\varepsilon_{\rm in}/\varepsilon_m$ and we have above introduced the shorthand notation $r_v^i(u_\pm)\equiv r_v(u_\pm,s;e_i^2)$ and $r_v^o(u_\pm)\equiv r_v(u_\pm,s;e_o^2)$. n_v^o is the standard depolarization factor for the v direction for the outer surface and satisfies the sum rule[23,24,27] $n_x^o+n_y^o+n_z^o=1$. We have also introduced

$$\rho_v \equiv \left(\frac{e_o}{e_i}\right)^{(u_+-u_-)}\frac{H_v^o(u_-)H_v^i(u_+)}{H_v^o(u_+)H_v^i(u_-)}, \tag{5}$$

where $H_v^o(u_\pm)\equiv H_v(u_\pm,s;e_o^2)$ and $H_v^i(u_\pm)\equiv H_v(u_\pm,s;e_i^2)$. We note that the total volume V_o only enters as a prefactor in the expression for α_{vv}. The geometry of the particle enters through the geometric entities n_v^o, $r_v^i(u_\pm)$, and $r_v^o(u_\pm)$. The standard isotropic depolarization factor n_v^o depends only on the shape (s and e_o^2), whereas $r_v^i(u_\pm)$ and $r_v^o(u_\pm)$ couple the geometry to the dielectric asymmetry of the coating. For an anisotropic coated sphere the expression for the polarizability agrees with the result obtained in Ref. 28. For an isotropic coating $\varepsilon_\parallel=\varepsilon_\perp$ the polarizability reduces to the standard result given in, for instance, Ref. 29. The imaginary part of α_{vv} is directly accessible through experimental extinction or absorption measurements. Explicitly, the extinction cross section is $\sigma_{vv}=\omega\,\mathrm{Im}[\alpha_{vv}]$, where $\mathrm{Im}[\cdot]$ denotes the imaginary part of the entity within the square brackets $[\cdot]$. In order to obtain the response of the coated metallic nanoparticle we must proceed by incorporating realistic microscopic dielectric functions for the coating and metal into expression (3) for the dipolar particle polarizability.

Let us consider the interior metallic region. In a standard fashion we assume that the dielectric function of the metal is described by a Drude function:

$$\varepsilon_{\rm in}(\omega) = \varepsilon_\infty - \frac{\omega_p^2}{\omega(\omega+i\Gamma_p)}, \tag{6}$$

with ω_p being the plasmon frequency, Γ_p is a phenomenological damping parameter, and ε_∞ is the dielectric function for large frequencies. We take $\varepsilon_\infty=1$ throughout this study. An *uncoated* metallic ellipsoidal particle in vacuum ($\epsilon_m=1$) has dipolar plasmon resonance frequencies

$$\omega_{pv} = \omega_p\sqrt{n_v^i}, \tag{7}$$

where n_v^i is the (purely geometric) depolarization factor of the inner ellipsoidal surface[23,27,29] (see also the Appendix).

We now give the dielectric function of the coating; we assume that the coating consists of molecules with dipolar polarizabilities which are diagonal but with different components in the normal and tangential directions; we denote the polarizabilities by $\gamma_\parallel$ ($\gamma_\perp$) [where a subscript $\perp$ ($\parallel$) denotes the polarizability component perpendicular (parallel) to the metallic surface normal]. Let us relate $\gamma_\parallel$ and $\gamma_\perp$ to the dielectric functions $\varepsilon_{c\parallel}(\omega)$ and $\varepsilon_{c\perp}(\omega)$ appearing in the coated ellipsoid polarizability α_{vv}: assuming that the surface is locally flat and imposing the conditions that the normal component of the total macroscopic electric field and the tangential component of the displacements field be continuous across the surface separating the molecular coating from the surrounding, we straightforwardly arrive at the following relation between the molecular polarizabilities and the coating dielectric functions:[30]

$$\varepsilon_\perp(\omega) = 1 + \frac{4\pi\gamma_\perp(\omega)}{v_0},$$

$$\varepsilon_\parallel(\omega)^{-1} = 1 - \frac{4\pi\gamma_\parallel(\omega)}{v_0}, \tag{8}$$

where v_0 is the unit cell volume per molecule.[24] Explicitly, we take the following form for the renormalized molecular polarizabilities:

$$\gamma_\mu(\omega) = \gamma_{\infty\mu} + (\gamma_{0\mu}-\gamma_{\infty\mu})\frac{\omega_{0\mu}^2}{\omega_{0\mu}^2-\omega^2-i\omega\Gamma_\mu}, \tag{9}$$

where $\gamma_{0\mu}$ is the static polarizability of the molecules, $\gamma_{\infty\mu}$ is the high-frequency polarizability, $\omega_{0\mu}$ is a resonance frequency, and Γ_μ is a damping parameter.[30,31] It is sometimes convenient to characterize the electromagnetic response properties of the coating by the effective oscillator strength (compare to Ref. 16), $c_{0\mu}=4\pi(\gamma_{0\mu}-\gamma_{\infty\mu})/v_0$, and the large frequency refractive indices $n_\perp=\varepsilon_{c\perp}(\omega=\infty)^{1/2}=(1+4\pi\gamma_{\infty\mu}/v_0)^{1/2}$ and $n_\parallel=\varepsilon_{c\parallel}(\omega=\infty)^{1/2}=(1-4\pi\gamma_{\infty\mu}/v_0)^{-1/2}$. We point out that the induced dipole coupling between molecules (and image dipoles in the metal), in general, introduce extra anisotropy by renormalizing the resonance frequencies, static polarizabilities, large frequency polarizabilities, and damping parameters compared to their "bare" values,[24,30,31] and all such anisotropies are included in expression (9).

To summarize, the general procedure for obtaining the polarizability $\alpha_{vv}(\omega)$ ($v=x,y,z$) for an ellipsoidal metallic nanoparticle coated with an anisotropic molecular layer is the following: Consider a nanoparticle with principal semiaxes a_x, a_y, and a_z. The size of the molecules together with these nanoparticle principal semiaxes determine the outer principal semiaxes b_x, b_y, and b_z; see Fig. 1. From these six principal semiaxes one calculates the the total volume V_o and the shape parameters s, e_i^2, and e_o^2 (for small coating thickness e_i^2 and e_o^2 are related through the relative coating thickness Δ_V). The problem is completed by specifying the metallic nanoparticle parameters in Eq. (6) and the renormalized

polarizability parameters of Eq. (9); alternatively, one may use experimental results for the nanoparticle and coating dielectric functions. Finally, the parameters above are used in the expression for $\alpha_{vv}(\omega)$ explicitly given in Eq. (3).

For the case where the coating resonance frequency $\omega_{0\mu}$ is close to being degenerate with one of the particle plasmon resonances [i.e., ω_{pv} of Eq. (7)] one expects hybridization between the two resonances.[3] In order to address this point we proceed by finding an approximate expression for the resonance frequencies for $\alpha_{vv}(\omega)$. Assuming a thin coating $\Delta_V \ll 1$ and utilizing the near-resonance approximation (the large-u result[23,24]) we obtain a simplified form for α_{vv}, as detailed in the Appendix. Below we use this α_{vv} for obtaining approximate expressions for the coupled (hybridized) resonance frequencies and for the extinction peak height at these resonances. The damping constants associated with the hybridized resonances are given in Eq. (A28). We point out the the approximate expressions for α_{vv} given in the Appendix are useful for investigating other quantities as well.

The resonance frequencies are obtained by finding the poles of α_{vv}; using the results in the Appendix, we find that resonances occur at frequencies $\omega=\omega_{v\mu}^{\pm}$ given by [see Eqs. (A12), (A13), (A18), and (A19)]

$$(\omega_{v\mu}^{\pm})^2 = \omega_{a\mu}^2 \pm (\omega_{d\mu}^4 + \omega_{0\mu}^4 D_{v\mu}^2)^{1/2}, \tag{10}$$

where, for brevity, we have introduced the notation $\omega_{a\mu}^2 = [(\omega_{pv}^o)^2 + \omega_{0\mu}^2]/2$ and $\omega_{d\mu}^2 = [(\omega_{pv}^o)^2 - \omega_{0\mu}^2]/2$, with $\omega_{pv}^o = \omega_p \sqrt{n_v^o}$; we have also introduced above a (dimensionless) parallel coupling strength

$$D_{v\parallel} = \left[\Delta_V g_{v\parallel} c_{0\parallel} (1 - n_v^o) \frac{\omega_p^2 - \omega_{a\parallel}^2}{\omega_{0\parallel}^2} \right]^{1/2} \tag{11}$$

and a perpendicular coupling strength

$$D_{v\perp} = \left[\Delta_V g_{v\perp} c_{0\perp} n_v^o \frac{\omega_{a\perp}^2}{\omega_{0\perp}^2} \right]^{1/2}, \tag{12}$$

with the effective oscillator strength $c_{0\mu} = 4\pi(\gamma_{0\mu} - \gamma_{\infty\mu})/v_0$ as defined before and the geometric factors defined as

$$g_{v\perp} = 1 - \frac{1}{F_o f_v^o}, \quad \text{and } g_{v\parallel} = \frac{1}{F_o f_v^o}, \tag{13}$$

where $f_v^o = f_v(s; e_o^2)$ so that $f_x^o = 1$, $f_y^o = 1 - s e_o^2$, $f_z^o = 1 - e_o^2$, and $F_o = 1 + (1 - s e_o^2)^{-1} + (1 - e_o^2)^{-1}$. The quantities $g_{v\mu}$ appear also in the polarizability for an anisotropic shell[24] and satisfy the three sum rules $g_{x\parallel} + g_{y\parallel} + g_{z\parallel} = 1$, $g_{x\perp} + g_{y\perp} + g_{z\perp} = 2$, and $g_{v\perp} + g_{v\parallel} = 1$. Equation (10) has the same form as that for two dipole coupled oscillators; see, for instance, Ref. 32 (also compare with Ref. 3). The strength of the molecular-plasmon interaction is characterized by the polarization- and molecular-orientation-dependent coupling strength $D_{v\mu}$, which depends on the relative coating volume parameter Δ_V and on the molecular response properties through $c_{0\mu}$, as well as on different geometric quantities.

For a *sphere* ($e_o^2 \to 0$) we have that $g_{v\parallel} = 1/3$, $g_{v\perp} = 2/3$, and $n_v^o = 1/3$ and Eqs. (11) and (12) become

$$D_{v\parallel}|_{\text{sph}} = \left[\Delta_V \frac{c_{0\parallel}}{27} \left(5 \frac{\omega_p^2}{\omega_{0\parallel}^2} - 3 \right) \right]^{1/2},$$

$$D_{v\perp}|_{\text{sph}} = \left[\Delta_V \frac{c_{0\perp}}{27} \left(\frac{\omega_p^2}{\omega_{0\perp}^2} + 3 \right) \right]^{1/2}. \tag{14}$$

The equations above quantify the degree of hybridization and its dependence on the molecular orientation for a coated metallic sphere.[33]

We notice from Eq. (10) that if the coating and particle plasmon resonance frequencies are well separated, in the sense $D_{v\mu}^2 \ll \omega_{d\mu}^4 / \omega_{0\mu}^4$, then the resonance frequencies are the uncoupled ones: ω_{pv} and $\omega_{0\mu}$.

In contrast, for $D_{v\mu}^2 \gg \omega_{d\mu}^4 / \omega_{0\mu}^4$, we have resonances approximately at

$$\omega_{v\mu}^{\pm} \approx \omega_{pv}^o (1 \pm D_{v\mu})^{1/2} \quad \text{for } \omega_{pv}^o = \omega_{0\mu} \tag{15}$$

and

$$D_{v\parallel} \approx (1 - n_v^o)(\Delta_V g_{v\parallel} c_{0\parallel} / n_v^o)^{1/2},$$

$$D_{v\perp} \approx (\Delta_V g_{v\perp} c_{0\perp} n_v^o)^{1/2}. \tag{16}$$

Thus, for $\omega_{pv}^o \approx \omega_{0\mu}$, we get $D_{v\mu} \propto \sqrt{\Delta_V}$ and we have strong hybridization between the nanoparticle and coating resonance frequencies, as will be illustrated in more detail in the next section. We also notice from Eq. (16) that for small n_v^o, $D_{v\parallel}$ can be substantially larger than $D_{v\perp}$, which can give a wider separation between $\omega_{v\parallel}^+$ and $\omega_{v\parallel}^-$ compared with that for $\omega_{v\perp}^{\pm}$.

The extinction peak height at one of the resonance frequency $\omega_{v\mu}^{\pm}$ is $\sigma_{vv}(\omega = \omega_{v\mu}^{\pm})$; using Eq. (A7), we convert this quantity into a scaled peak height $T_{v\mu}^{\pm} = 4\pi\sigma_{vv}(\omega_{v\mu}^{\pm}) / [V_o (\omega_{v\mu}^{\pm})^2]$ at the resonances. Employing the thin-coating approximation and assuming that we are close to a resonance Eqs. (A14) and (A20) apply; i.e., we have the approximate result

$$T_{v\mu}^{\pm} = \frac{\omega_p^2}{(\omega_{v\mu}^{\pm})^2} \times \frac{\omega_{0\mu}^2 - (\omega_{v\mu}^{\pm})^2}{\Gamma_p (\omega_{0\mu}^2 - (\omega_{v\mu}^{\pm})^2) + \Gamma_\mu ((\omega_{pv}^o)^2 - (\omega_{v\mu}^{\pm})^2)}, \tag{17}$$

which for $\omega_{pv}^o \approx \omega_{0\mu}$ gives

$$T_{v\mu}^{\pm} = \frac{1}{n_v^o (\Gamma_p + \Gamma_\mu)} \frac{1}{1 \pm D_{v\mu}}, \tag{18}$$

with $D_{v\mu}$ given by Eq. (16).

For the case of an uncoated metallic nanoparticle the scaled peak height takes the form $T_{vp} = 1/(n_v^o \Gamma_p)$ [see Eq. (A8)]. Equation (18) shows that at strong coupling (i.e., for $\omega_{pv}^o \approx \omega_{0\mu}$), $T_{v\mu}^{\pm}$ are of the same order of magnitude as T_{vp}.

For a very thin coating without any interior metal we have $T_{v\mu}(\varepsilon_i = 1) \approx \Delta_V g_{v\mu} c_{0\mu} / \Gamma_\mu$ [see Eqs. (A11) and (A17) and Ref. 24], which is much smaller than T_{vp}. Comparing with Eq. (17) we notice that $T_{v\mu}^{\pm} / T_{v\mu}(\varepsilon_i = 1) \propto (\Delta_V)^{-1}$ (note, however, that $\omega_{v\mu}^{\pm}$ depends on Δ_V), revealing substantial surface enhancement (see next section).

III. RESULTS AND DISCUSSIONS

In the following, we illustrate the electromagnetic response properties of a coated metallic nanoparticle via the extinction cross section $\sigma_{vv}=\omega\,\mathrm{Im}[\alpha_{vv}]$ for the case of a prolate ($a_y=a_z$—i.e., $s=1$, "cigar-shaped") spheroid. We consider two different situations: the case when the molecules in the coating have their "resonant" axes (i) parallel and (ii) perpendicular to the surface normal. The polarizability component along the resonant axis is $\alpha_\parallel$ in case (i) and $\alpha_\perp=\alpha_\parallel/2$ in case (ii), which corresponds to coatings with identical but differently oriented molecules. For each of the two cases, the external field $\vec{E}_0$ is applied either along the long axis (x axis) or the short axis (y or z axis).

In Fig. 1(b), the polarization-averaged extinction cross section for an *uncoated* metallic spheroid is shown together with the cross section for an spheroidally shaped molecular layer *without* an interior nanoparticle and with the resonant transition dipole moments oriented in the parallel and perpendicular directions. There are two plasmon peaks, as expected for a spheroidal metal particle (two of the principal axes equal), with resonance wavelengths to the red ($\vec{E}_0\|x$ axis) and to the blue ($\vec{E}_0\|y$, z axes) of the familiar LSP resonance of a sphere ($\lambda/\lambda_p=\sqrt{3}\approx 1.73$). The extinction peaks of the molecular layer are about 50 times weaker than the plasmons for both molecular orientations. Notice that, for geometric reasons, the extinction peak height for the molecular layer is smallest for the case where the external field is in the x direction, with the molecules oriented in the parallel direction; see Ref. 24 for a thorough discussion of geometric- and molecular-orientation-dependent effects in the response of an ellipsoidal molecular layer. Also notice the small difference in peak position between cases (i) and (ii); in Ref. 24, it was shown that for $\Delta_V \ll 1$ there are no curvature-induced shifts for the molecular layer resonance frequencies (see also the Appendix). Here, Δ_V is not sufficiently small and there are some minor shifts of the resonance frequencies.

In Fig. 2, we show extinction spectra corresponding to the full coated spheroid response problem for the four distinct cases mentioned above—i.e., molecular orientation perpendicular (a), (b) or parallel (c), (d) to the surface normal and incident field parallel to the short (a), (c) or long (b), (d) spheroid axes. The different colors of the curves correspond to different coating resonance frequencies $\omega_{0\mu}$. It is clear that there is strong hybridization between the coating and plasmon resonances whenever $\omega_{0\mu}\approx\omega_{pv}$ ($\mu=\|,\perp$ and $v=x,y,z$) in all cases. However, the degree of hybridization differs greatly between the different molecular orientations and polarization configurations.

In order to investigate the peak height of the resonances (see Fig. 2), Fig. 3 shows the scaled peak height $T^{\pm}_{v\mu}$ [defined in Eq. (A7)] compared to the scaled peak height $T_{v\mu}(\varepsilon_i=1)$ for a molecular layer (obtained from Fig. 1) for different coating resonance frequencies. A comparison to the result given in Eq. (17) is also made. We notice the two coupled resonances obtain similar peak heights as $\omega_{0\mu}$ approaches the particle plasmon frequency ω_{pv}. We also point out that the approximate expression, Eq. (17), works surprisingly well, considering that it is based on a close-to-resonance and thin-coating approximation, even far off the resonances.

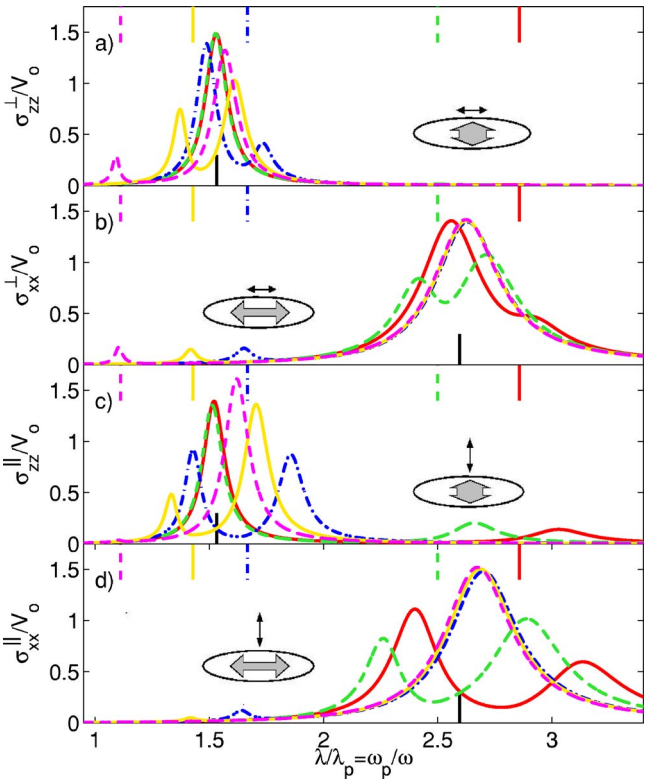

FIG. 2. (Color online) Extinction spectrum for a coated prolate spheroid with different orientations of the molecules on the surface. The spectrum is in units of the total volume V_o of the coated spheroid. $\sigma^{\mu}_{vv}=\omega\,\mathrm{Im}[\alpha_{vv}]$ ($\mu=\|,\perp$ and $v=x,z$) and $\lambda=2\pi c/\omega$ is the wavelength of the external electromagnetic field. (a) The external field is along the z axis (short axis) of the spheroid. The molecules have their resonant axes *perpendicular* to the metallic particle normal. (b) The external field is along the x axis (long axis), and the molecules are *perpendicular* to the layer normal. (c) The field is along the z axis, and the molecules have their resonant axis *parallel* to the layer normal. (d) The field is along the x axis, and the molecules are oriented *parallel* to the layer normal. The different colors are the spectra for different molecular resonant wavelengths; the upper vertical bars indicate these resonance wavelengths $\lambda_{0\mu}=2\pi c/\omega_{0\mu}$. Here, we chose the following values for $\omega_{0\mu}$: $0.35\omega_p$, $0.4\omega_p$, $0.6\omega_p$, $0.7\omega_p$, $0.9\omega_p$. The lower vertical bar is the particle plasmon resonance wavelengths $\lambda_{pv}=2\pi c/\omega_{pv}$ ($v=x,z$). The same parameters as in Fig. 1 were used. Notice the strong hybridization when $\lambda_{0\mu}\approx\lambda_{pv}$ and increased peak height (surface enhanced absorption) for the molecular resonance, compared with Fig. 1(b).

When the molecular resonance is far above or far below a plasmon resonance, we have a situation that can best be described as surface-enhanced absorption from the molecular layer;[18] i.e., the magnitude of the molecular resonance peak is greatly enhanced but its position and width are not changed dramatically from the case of a "free" molecular layer (see Figs. 2 and 3). In this regime, the particle plasmons (at λ_{pv}, with $v=x,y,z$) become either redshifted or blueshifted relative to the uncoated metallic spheroid resonance wavelength depending on the molecular resonance wavelength λ_0. Interestingly, the enhanced absorption from

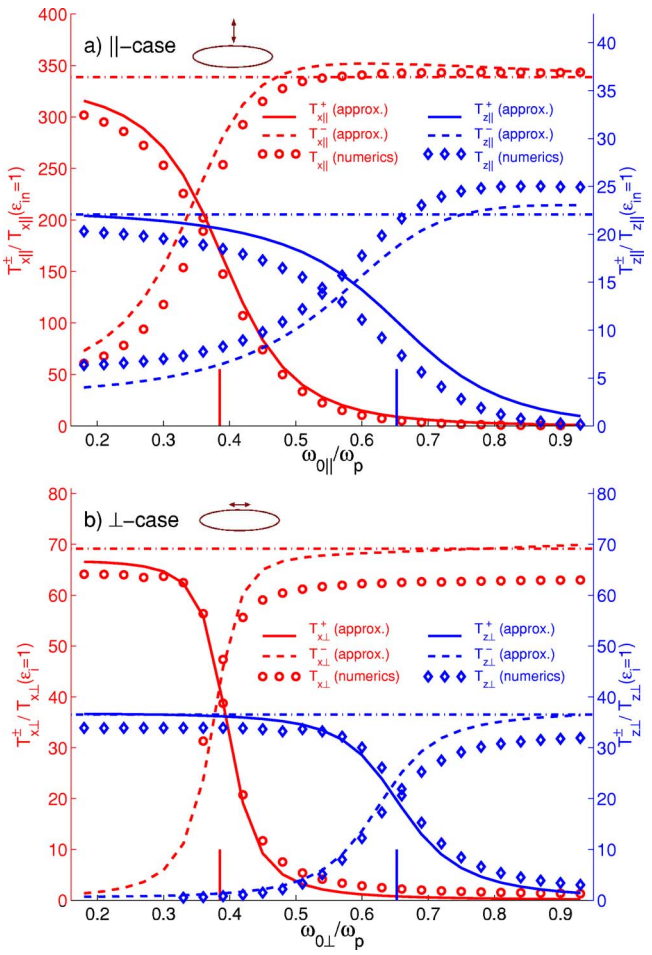

FIG. 3. (Color online) Scaled peak height for the coupled resonances in a coated prolate metal spheroid for the case (a) when the coating molecules have their resonant axis *parallel* to the surface normal and (b) for a *perpendicular* resonance. The resonance frequencies $\omega^{\pm}_{v\mu}$ and peak heights $\sigma_{vv}(\omega^{\pm}_{v\mu})$, see Figs. 2 and 4, for different $\omega_{0\mu}$ were numerically determined and used to calculate the scaled peak height $T^{\pm}_{v\mu}=4\pi\sigma_{vv}(\omega^{\pm}_{v\mu})/[V_o(\omega^{\pm}_{v\mu})^2]$ ($v=x,z$ and $\mu=\|,\perp$); see Eq. (A7). The peak heights were normalized by the molecular layer peak heights $T_{v\mu}(\varepsilon_i=1)$ obtained from Fig. 1. The vertical solid lines correspond to the two plasmon resonances ω_{px} and ω_{pz}, Eq. (7). The dash-dotted horizontal lines correspond to the plasmon peak heights as given in the text right after Eq. (17). The solid and dashed curves are the approximate results given in Eq. (17). The same parameters as in Fig. 1 were used. Notice the different ranges of the ordinates and that the abscissas are in frequency units.

the molecular layer is not symmetric on the two sides of the plasmon. This can be seen when comparing Figs. 2(a) and 2(c) (see also Fig. 3), corresponding to polarization along the short axis of the spheroid. When the molecular resonance is far to the red of the plasmon, absorption enhancement is seen for the case when the molecular resonance axis is parallel to the surface normal [Fig. 2(c)], but not for the perpendicular case [Fig. 2(a)]. The situation is reversed (although less pronounced) when the molecular resonance is to the blue of the plasmon; i.e., absorption enhancement occurs for the perpendicular but not for the parallel case. Similar effects are seen in Figs. 2(b) and 2(d), corresponding to polarization along the long axis. From Fig. 3(a) we notice that particularly strong surface enhancement (roughly a factor of 50 for the extinction cross section for the parameters used here) occurs to the red of the plasmon for the parallel case with the incident field along the x axis.

The differences above can be understood as follows: To the red of a plasmon resonance, the induced field from the particle is in phase with the applied field and normal to the surface at the poles of the particle (where the poles are defined by the direction of the induced dipole), resulting in enhanced absorption from molecules oriented parallel the surface normal. Molecules with the perpendicular orientation instead couple mainly to the total field around the equator of the particle, where the field is perpendicular to the surface normal. But to the red this field is weak, because here the induced field is out of phase with the applied field. Hence, there is very little enhanced absorption to the red of the plasmon in Fig. 2(a) but a large enhancement in Fig. 2(c). The same type of arguments applies to the case when the molecular resonance is to the blue of the plasmon, but here the situation becomes reversed because the induced particle dipole is out of phase with the incident field.[35]

The case when the molecular resonance is degenerate with one of the plasmons corresponds to a regime that cannot be described in terms of enhanced absorption. Instead, we have two completely hybridized resonances that exhibit "avoided crossing," analogous to the case of two strongly coupled (quantum or classical) harmonic oscillators, as is seen in Eq. (10). Figure 4 illustrates this behavior for the two molecular orientations considered. In the vocabulary of Ref. 3, the high-frequency modes $\omega^{+}_{v\mu}$ in Eq. (10) correspond to "antibonding" combinations—i.e., the case where the induced dipole on the particle is out of phase with the molecular transition dipoles—while the "bonding" modes $\omega^{-}_{v\mu}$ correspond to the case when the excitations are in phase. This corresponds to Rabi oscillations in which the excitation energy oscillates back and forth between the plasmonic particle and the molecular layer. As can be seen in Fig. 4, the mode splitting is much more significant when the molecular resonance is oriented parallel to the surface normal [Fig. 4(a)] than for the perpendicular [Fig. 4(b)] case. This difference simply reflects the predominant polarization of the local field at the surface (the field would be strictly parallel to the surface normal for a perfect conductor at zero frequency). We also note that the splitting (expressed in frequency units) is larger for the plasmon that corresponds to polarization along the short axis of the prolate spheroid for both molecular orientations, which is somewhat surprising considering that the field enhancement is highest at the sharp ends of the spheroid.[35] However, the coupling strength is determined by the surface-integrated local field at the two plasmon resonance frequencies, and for geometric reasons this quantity is higher for the doubly degenerate short-axis plasmon in the present case.

To the best of our knowledge, there are no experimental studies that have directly probed the orientation-dependent plasmon-molecule coupling discussed here. However, the advanced nanofabrication and molecular functionalization technologies of today clearly make such studies a realistic pos-

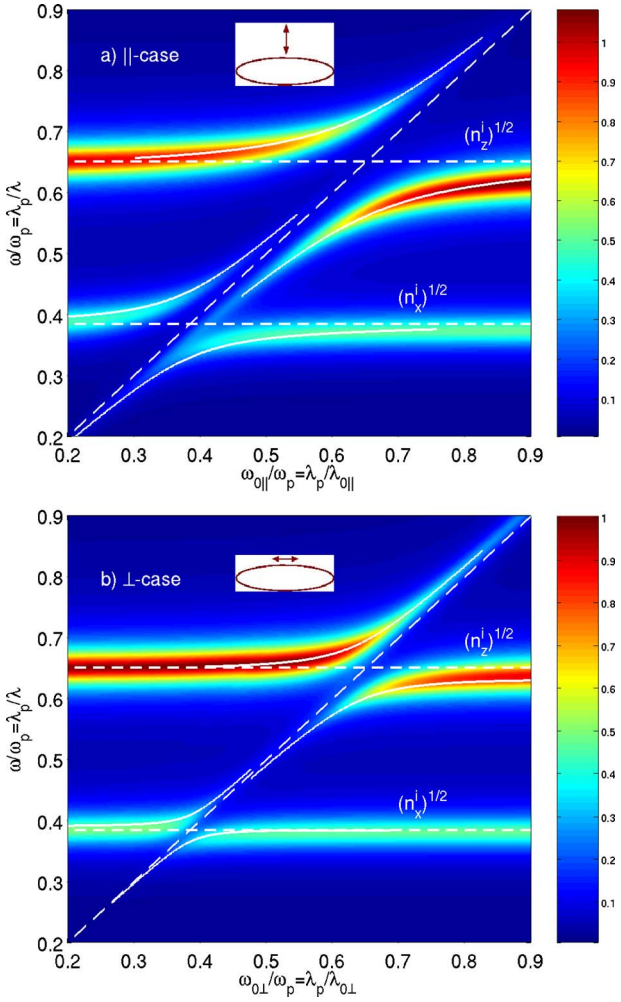

FIG. 4. (Color online) Illustration of strong coupling and "avoided crossing" between the plasmonic and molecular resonances of a coated prolate metal spheroid for the case (a) when the molecules have their resonant axis *parallel* to the surface normal and (b) for a *perpendicular* resonance. The horizontal dashed lines correspond to the two plasmon resonances ω_{px} and ω_{pz}, and the diagonal dashed lines denotes $\omega=\omega_{0\mu}$. The solid white curves are the approximate results for the coupled resonances as given in Eq. (10). The same parameters as in Fig. 1 were used. Notice that the axes are in frequency units.

sibility. One of the most interesting options could be to use a plasmonic nanoparticle covered by an ordered layer of chromophores as a nanoscopic bio-chemo sensor. For example, it can be expected that the exact orientation of the chromophores on the surface will be sensitive to *p*H and to the interaction with molecules in solution. The chromophores might also be incorporated as functional groups into larger biomacromolecules that change the orientation and conformation upon biorecognition reaction with an analyte. Such sensing reactions would then affect the coupling between the surface plasmons and the chromophores, giving rise to pronounced changes in the extinction or scattering spectrum of the composite nanoparticle. To illustrate this possibility, Fig. 5 shows the difference spectra between the parallel and perpendicular orientations discussed above. As expected, the

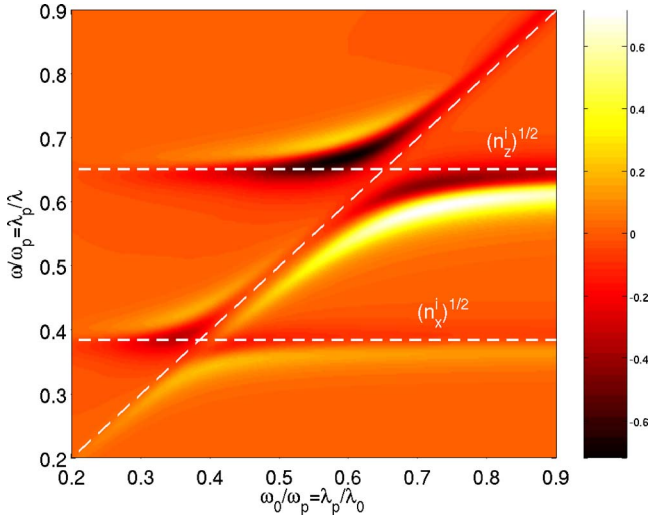

FIG. 5. (Color online) Difference in averaged extinction cross section, $\Delta\sigma/V_o=(\sigma^{\|}-\sigma^{\perp})/V_o$ (indicated by the different colors), between the parallel and perpendicular cases as shown in Figs. 4(a) and 4(b), as a function molecular resonance frequency $\omega_0=\omega_{0\|}=\omega_{0\perp}$ and external field frequency ω. Note that the axes are in frequency units.

difference is largest for molecular resonance wavelengths that overlap the LSP modes. However, a noticeable difference is observed even far off the plasmon resonances, indicating that molecular orientation effects needs to be taken into account also in classical nanoparticle refractive index sensing experiments.

IV. SUMMARY

We have described an analytic method for calculating the optical response of arbitrary ellipsoidal nanoparticles with anisotropic molecular coatings in the small-particle limit and applied this theory to the case of a prolate metal spheroid covered with chromophores. The results show that the hybridization between the molecular resonance and the localized plasmon resonances of the nanoparticle is highly anisotropic. It is suggested that this sensitivity can be utilized for novel bio- and chemo-sensing applications that are based on molecular orientation rather than refractive index contrast.

ACKNOWLEDGMENTS

M.K. acknowledges stimulating discussions with Peter Nordlander and Texas Instruments, which supported part of this work. G.M. acknowledges the hospitality of the Department of Applied Physics, Chalmers University. This work was financially supported by the Swedish Research Council.

APPENDIX: APPROXIMATE EXPRESSION FOR COUPLED RESONANCES AND PEAK HEIGHTS AND WIDTHS

In this appendix we use the large-u (close to a resonance) and thin-coating approximations for the coated ellipsoid polarizability given in Eq. (3) in order to derive approximate

expressions for the coupled resonance frequencies as well as for the peak heights and widths of these excitations.

Close to a resonance (u large) and for a thin coating ($\Delta_V \ll 1$) we have that Eq. (3) becomes

$$\alpha_{vv} = \frac{V_o}{4\pi n_v^o} \frac{J_v(\kappa=-1)}{J_v(\kappa=1/n_v^o-1)}, \tag{A1}$$

with

$$J_v(\kappa) = \varepsilon_i + \kappa + \Delta_V g_{v\perp}\varepsilon_\perp + \Delta_V \varepsilon_i g_{v\|}\varepsilon_\|^{-1}\kappa, \tag{A2}$$

in an identical fashion as the derivation given in Ref. 24. The geometric factors $g_{v\|}$ and $g_{v\perp}(v=x,y,z)$ are given in Eq. (13). Explicit expressions for the dielectric functions ε_i, $\varepsilon_\perp$, and $\varepsilon_\|$ appearing in Eq. (A2) are given in Eqs. (6) and (8). Below we investigate $J_v(\kappa)$ in the limits of (subsection 1) no coating $\Delta_V=0$, (subsection 2) external field frequency close to the parallel resonance frequency, $\omega \approx \omega_{0\|}$; (subsection 3) external field frequency close to the perpendicular resonance frequency, $\omega \approx \omega_{0\perp}$. In subsection 4 we derive expressions for the peak widths of the hybridized resonances.

No coating, $\Delta_V=0$

For the case of no coating, $\Delta_V=0$, we have that $J_v(\kappa) = \varepsilon_i + \kappa$ and therefore the polarizability, Eq. (A1), can be written

$$\alpha_{vv}(\omega) = \frac{V_o}{4\pi n_v^o} \frac{K_v(\kappa=-1)}{K_v(\kappa=1/n_v^o-1)}, \tag{A3}$$

where K_v equals J_v multiplied a by a factor independent of κ and, explicitly,

$$\begin{aligned} \mathrm{Re}[K_v(\kappa)] &= \omega_p^2 - \omega^2(1+\kappa), \\ \mathrm{Im}[K_v(\kappa)] &= -\omega\Gamma_p(1+\kappa), \end{aligned} \tag{A4}$$

with $\mathrm{Re}[\cdot](\mathrm{Im}[\cdot])$ denoting the real (imaginary) part of the entity inside $[\cdot]$. The resonance criterion $\mathrm{Re}[K_v(\kappa=1/n_v^o-1)]=0$ gives, together with Eq. (A4), the uncoated metallic ellipsoid resonance frequencies:

$$\omega_{\mathrm{res},v}^2 = (\omega_{pv}^o)^2 = \omega_p^2 n_v^o, \tag{A5}$$

in agreement with Eq. (7) as it should (note that when $\Delta_V=0$, then $n_v^i=n_v^o$). At one of the resonances the extinction peak height $\sigma_{vv}(\omega_{\mathrm{res},v}) = \omega_{\mathrm{res},v}\,\mathrm{Im}[\alpha_{vv}(\omega_{\mathrm{res},v})]$ is

$$\begin{aligned} \sigma_{vv}(\omega_{\mathrm{res},v}) &= -\frac{V_o}{4\pi n_v^o} \left.\frac{\omega\,\mathrm{Re}[K_v(\kappa=-1)]}{\mathrm{Im}[K_v(\kappa=1/n_v^o-1)]}\right|_{\omega=\omega_{\mathrm{res},v}} \\ &= \frac{V_o}{4\pi n_v^o}\Gamma_p^{-1}\omega_{\mathrm{res},v}^2, \end{aligned} \tag{A6}$$

where we have used Eq. (A4) and $\omega_{\mathrm{res},v}$ is given in Eq. (A5). It is convenient to define a scaled peak height

$$T_v \equiv \frac{4\pi}{V_o}\frac{\sigma_{vv}(\omega_{\mathrm{res},v})}{\omega_{\mathrm{res},v}^2}, \tag{A7}$$

so that, using Eq. (A6), we have

$$T_v = T_{vp} = \frac{1}{n_v^o \Gamma_p}. \tag{A8}$$

Thus, for an uncoated nanoparticle T_v is a measure of the lifetime (inverse damping) of the plasmon excitation. We will below use the definition, Eq. (A7), to compute approximate scaled peak heights of the coated metallic ellipsoid excitations.

$\omega \approx \omega_{0\|}$

For the case $\omega \approx \omega_{0\|}$ (and $\omega_{0\|} \neq \omega_{0\perp}$) we neglect the "perpendicular" term in Eq. (A2), so that $J_v(\kappa) = \varepsilon_i + \kappa + \Delta_V \varepsilon_i g_{v\|}\varepsilon_\|^{-1}\kappa$. Using the explicit expressions for the dielectric functions described by Eqs. (6) and (8) along with Eq. (9) we find

$$\begin{aligned} K_v(\kappa) &= [\omega(\omega+i\Gamma_p)(\omega^2-\omega_{0\|}^2+i\omega\Gamma_\|)]J_v(\kappa) \\ &\approx (\omega^2+i\omega\Gamma_p-\omega_p^2)(\omega^2-\omega_{0\|}^2+i\omega\Gamma_\|) \\ &\quad + (\omega^2+i\omega\Gamma_p-\omega_p^2)\Delta_V g_{v\|}c_{0\|}\omega_{0\|}^2\kappa \\ &\quad + (\omega^2+i\omega\Gamma_p)(\omega^2-\omega_{0\|}^2+i\omega\Gamma_\|)\kappa. \end{aligned} \tag{A9}$$

Assuming that $\Delta_V \ll 1$ and neglecting terms of order $\Gamma^2(\Gamma = \Gamma_p, \Gamma_\|)$ and $\Gamma\Delta_V$ (the neglected term $\Delta_V g_{v\perp}\varepsilon_\perp$ is of the same order as the terms neglected here) we find that the polarizability can be written in the same form as in Eq. (A3) now with

$$\begin{aligned} \mathrm{Re}[K_v(\kappa)] &= (\omega_{0\|}^2-\omega^2)[\omega_p^2-\omega^2(1+\kappa)] \\ &\quad - \Delta_V g_{v\|}c_{0\|}\omega_{0\|}^2(\omega_p^2-\omega^2)\kappa, \\ \mathrm{Im}[K_v(\kappa)] &= -\omega(\Gamma_p(\omega_{0\|}^2-\omega^2)(1+\kappa) + \Gamma_\|(\omega_p^2-\omega^2(1+\kappa))). \end{aligned} \tag{A10}$$

We notice that the second term in the expression for $\mathrm{Re}[K_v(\kappa)]$ cannot be discarded because the first term may be close to zero. In the limit $\Delta_V, \Gamma_\| \to 0$ the polarizability reduces to the uncoated result from the previous subsection.

In the limit $\omega_p, \Gamma_p \to 0$ (i.e., $\varepsilon_i = \varepsilon_\infty = 1$) we recover, to lowest order in Δ_V, the result in Ref. 24:

$$\alpha_{vv}(\omega) = \Delta_V \frac{V_o}{4\pi} g_{v\|}c_{0\|}\frac{\omega_{0\|}^2}{\omega_{0\|}^2-\omega^2-i\omega\Gamma_\|}, \tag{A11}$$

as it should.

Turning back to the general expression, Eq. (A10), we find that the resonance condition $\mathrm{Re}[K_v(\kappa=1/n_v^o-1)]=0$ gives resonance frequencies

$$(\omega_{v\|}^\pm)^2 = \frac{\omega_p^2 n_v^o + \omega_{0\|}^2}{2} \pm \left[\left(\frac{\omega_p^2 n_v^o - \omega_{0\|}^2}{2}\right)^2 + \omega_{0\|}^4 D_{v\|}^2\right]^{1/2}, \tag{A12}$$

with a dimensionless coupling strength $D_{v\|}$ defined by

$$D_{v\|}^2 = \Delta_V g_{v\|}c_{0\|}(1-n_v^o)\left(\frac{\omega_p^2}{\omega_{0\|}^2} - \frac{\omega_p^2 n_v^o + \omega_{0\|}^2}{2\omega_{0\|}^2}\right). \tag{A13}$$

Using Eq. (A7) we find that the scaled peak height $T^{+}_{v\|}(T^{-}_{v\|})$ of the resonance characterized by resonance frequency $\omega^{+}_{v\|}(\omega^{-}_{v\|})$ becomes (for $\omega_p \neq 0$)

$$T^{\pm}_{v\|} = \frac{\omega_p^2}{(\omega^{\pm}_{v\|})^2} \times \frac{(\omega_{0\|}^2 - (\omega^{\pm}_{v\|})^2)}{\Gamma_p(\omega_{0\|}^2 - (\omega^{\pm}_{v\|})^2) + \Gamma_{\|}(\omega_p^2 n_v^o - (\omega^{\pm}_{v\|})^2)}, \tag{A14}$$

where we have used the fact that $(\omega^{\pm}_{v\|})^2$ is of the order $(\Delta_V)^{1/2}$ and neglected terms of order Δ_V.

We notice from Eq. (A12) that if $D_{v\|} \ll |[\omega_p^2 n_v^o - \omega_{0\|}^2]/[2\omega_{0\|}^2]|$, then the resonance frequencies are the uncoupled ones: $\omega_p\sqrt{n_v^o}$ and $\omega_{0\|}$.

If instead $D_{v\|} \gg |[\omega_p^2 n_v^o - \omega_{0\|}^2]/[2\omega_{0\|}^2]|$ (i.e., for $\omega_p^2 n_v^o \approx \omega_{0\|}^2$), we get $(\omega^{\pm}_{v\|})^2 \approx \omega_p^2 n_v^o[1 \pm D_{v\|}]$ and

$$T^{\pm}_{v\|} = \frac{1}{n_v^o(\Gamma_p + \Gamma_{\|})} \frac{1}{1 \pm D_{v\|}}, \tag{A15}$$

with $D_{v\|} = (\Delta_V g_{v\|} c_{0\|}(1 - n_v^o)^2/n_v^o)^{1/2}$, showing strong hybridization of the plasmon and coating resonances.

$\omega \approx \omega_{0\perp}$

For the case $\omega \approx \omega_{0\perp}$ (and $\omega_{0\|} \neq \omega_{0\perp}$) we neglect the "parallel" term in Eq. (A2), so that $J_v(\kappa) = \varepsilon_i + + \kappa + \Delta_V g_{v\perp}\varepsilon_{\perp}$. Using the explicit expressions for the dielectric functions in Eqs. (6) and (8) along with Eq. (9) an identical analysis as in the preceding subsection shows that polarizability can be written in the same form as in Eq. (A3) with

$$\mathrm{Re}[K_v(\kappa)] = (\omega_{0\perp}^2 - \omega^2)[\omega_p^2 - \omega^2(1+\kappa)] - \Delta_V g_{v\perp} c_{0\perp} \omega_{0\perp}^2 \omega^2,$$

$$\mathrm{Im}[K_v(\kappa)] = -\omega(\Gamma_p(\omega_{0\perp}^2 - \omega^2)(1+\kappa) + \Gamma_{\perp}(\omega_p^2 - \omega^2(1+\kappa))). \tag{A16}$$

In the limit $\Delta_V, \Gamma_{\perp} \to 0$ we recover the uncoated result.

In the limit $\omega_p, \Gamma_p \to 0$ (i.e., $\varepsilon_i = \varepsilon_{\infty} = 1$) we obtain, to lowest order in Δ_V,

$$\alpha_{vv} = \Delta_V \frac{V_o}{4\pi} g_{v\perp} c_{0\perp} \frac{\omega_{0\perp}^2}{\omega_{0\perp}^2 - \omega^2 - i\omega\Gamma_{\perp}}, \tag{A17}$$

in agreement with the result in Ref. 24.

The resonance condition $\mathrm{Re}[K_v(\kappa = 1/n_v^o - 1)] = 0$ gives resonance frequencies

$$(\omega^{\pm}_{v\perp})^2 = \frac{\omega_p^2 n_v^o + \omega_{0\perp}^2}{2} \pm \left[\left(\frac{\omega_p^2 n_v^o - \omega_{0\perp}^2}{2}\right)^2 + \omega_{0\perp}^4 D_{v\perp}^2\right]^{1/2}, \tag{A18}$$

with the dimensionless coupling strength $D_{v\perp}$ defined by

$$D_{v\perp}^2 = \Delta_V g_{v\perp} c_{0\perp} n_v^o \left(\frac{\omega_p^2 n_v^o + \omega_{0\perp}^2}{2\omega_{0\perp}^2}\right); \tag{A19}$$

compare to Eq. (A13).

The scaled peak height $T^{+}_{v\perp}(T^{-}_{v\perp})$ of the resonance characterized by resonance frequency $\omega^{+}_{v\perp}(\omega^{-}_{v\perp})$ is obtained from Eq. (A7). We find (for $\omega_p \neq 0$)

$$T^{\pm}_{v\perp} = \frac{\omega_p^2}{(\omega^{\pm}_{v\perp})^2} \times \frac{\omega_{0\perp}^2 - (\omega^{\pm}_{v\perp})^2}{\Gamma_p(\omega_{0\perp}^2 - (\omega^{\pm}_{v\perp})^2) + \Gamma_{\perp}(\omega_p^2 n_v^o - (\omega^{\pm}_{v\perp})^2)}, \tag{A20}$$

in the same manner as in the preceding subsection.

We notice now from Eq. (A18) that if $D_{v\perp} \ll |[\omega_p^2 n_v^o - \omega_{0\perp}^2]/[2\omega_{0\perp}^2]|$, then the resonance frequencies are the uncoupled ones: $\omega_p\sqrt{n_v^o}$ and $\omega_{0\perp}$.

If instead $D_{v\perp} \gg |[\omega_p^2 n_v^o - \omega_{0\perp}^2]/[2\omega_{0\perp}^2]|$ (i.e., for $\omega_p^2 n_v^o \approx \omega_{0\perp}^2$), we get $(\omega^{\pm}_{v\perp})^2 \approx \omega_p^2 n_v^o[1 \pm D_{v\perp}]$ and

$$T^{\pm}_{v\perp} = \frac{1}{n_v^o(\Gamma_p + \Gamma_{\perp})} \frac{1}{1 \pm D_{v\perp}}, \tag{A21}$$

with $D_{v\perp} = (\Delta_V g_{v\perp} c_{0\perp} n_v^o)^{1/2}$, showing again strong hybridization of the plasmon and coating resonances.

Damping constants

In the preceding subsections we derived expression for the resonance frequencies and peak heights for the coating-nanoparticle-hybridized resonances. We here proceed by also deriving expressions for the damping constants (inverse lifetimes), which determine the peak *widths*. It is convenient to define

$$\Delta\omega^2 \equiv (\omega^{\pm}_{v\mu})^2 - \omega^2, \tag{A22}$$

where $\omega^{\pm}_{v\mu}$ are the resonance frequencies; see Eqs. (A12) and (A18). We can then expand $K_v(\kappa)$ in Eq. (A3) according to

$$K_v(\kappa) = K_v^{(0)}(\kappa) + \Delta\omega^2 K_v^{(1)}(\kappa) + \cdots, \tag{A23}$$

where $K_v^{(0)}(\kappa) = K_v(\kappa)|_{\omega = \omega^{\pm}_{v\mu}}$. Inserting this expansion into the expression for the polarizability, Eq. (A3), using the resonance condition $\mathrm{Re}[K_v(\kappa = 1/n_v^o - 1)] = 0$, and keeping only terms to lowest order in $\Delta\omega^2$ we find

$$\alpha_{vv}(\omega \sim \omega^{\pm}_{v\mu}) \approx \frac{V_o}{4\pi n_v^o} \frac{\mathrm{Re}[K_v^{(0)}(-1)] + i\,\mathrm{Im}[K_v^{(0)}(-1)]}{\Delta\omega^2\,\mathrm{Re}[K_v^{(1)}(1/n_v^o - 1)] + i\,\mathrm{Im}[K_v^{(0)}(1/n_v^o - 1)]}. \tag{A24}$$

By furthermore neglecting the imaginary part in the numerator (i.e., assuming small damping) we find

$$\alpha_{vv}(\omega \sim \omega^{\pm}_{v\mu}) \approx \frac{V_o}{4\pi n_v^o} \frac{\mathrm{Re}[K_v^{(0)}(-1)]}{(\omega^{\pm}_{v\mu})^2\,\mathrm{Re}[K_v^{(1)}(1/n_v^o - 1)]} \times \frac{(\omega^{\pm}_{v\mu})^2}{(\omega^{\pm}_{v\mu})^2 - \omega^2 - i\omega\Gamma^{\pm}_{v\mu}}, \tag{A25}$$

where we introduced the damping constant

$$\Gamma^{\pm}_{v\mu} = \frac{\mathrm{Im}[K_v^{(0)}(1/n_v^o - 1)]}{\omega^{\pm}_{v\mu}\,\mathrm{Re}[K_v^{(1)}(1/n_v^o - 1)]}. \tag{A26}$$

In order to obtain an explicit expression for the damping we proceed by expanding Eqs. (A10) and (A16) and obtain

$$\mathrm{Re}[K_v^{(1)}(1/n_v^o - 1)] = \frac{2}{n_v^o}[\omega_{a\mu}^2 - (\omega_{v\mu}^{\pm})^2], \qquad \text{(A27)}$$

where $\omega_{a\mu}^2 = (\omega_{0\mu}^2 + \omega_p^2 n_v^o)/2$ and we neglected terms of order $\Delta_V \Delta\omega^2$. Combining Eqs. (A26) and (A27) we finally find that the damping constant takes the form

$$\Gamma_{v\mu}^{\pm} = \frac{\Gamma_p(\omega_{0\mu}^2 - (\omega_{v\mu}^{\pm})^2) + \Gamma_\mu(\omega_p^2 n_v^o - (\omega_{v\mu}^{\pm})^2)}{2[\omega_{a\mu}^2 - (\omega_{v\mu}^{\pm})^2]}. \qquad \text{(A28)}$$

Concluding, we above showed that close to one of the resonances the polarizability can be approximated by a Lorentzian [see Eqs. (A25)] with a width determined by Eq. (A28).

Using Eqs. (A25), (A27) and the definition, Eq. (A7), we find the following relation between the scaled peak height and the damping constant:

$$T_{v\mu}^{\pm} = \frac{\omega_p^2}{2(\omega_{v\mu}^{\pm})^2} \frac{\omega_{0\mu}^2 - (\omega_{v\mu}^{\pm})^2}{\omega_{a\mu}^2 - (\omega_{v\mu}^{\pm})^2} \frac{1}{\Gamma_{v\mu}^{\pm}}, \qquad \text{(A29)}$$

to lowest order in Δ_V; compare Eq. (A8). Inserting Eq. (A28) into the equation above we recover the results in Eqs. (A14) and (A20), as it should.

*Corresponding author; Email address: ambjorn@nordita.dk

[1] U. Kreibig and M. Vollmer, *Optical Properties of Metal Clusters* (Springer-Verlag, Berlin, 1995).

[2] J. Prikulis, P. Hanarp, L. Olofsson, D. Sutherland, and M. Käll, Nano Lett. **4**, 1003 (2004).

[3] E. Prodan, C. Radloff, N. J. Halas, and P. Nordlander, Science **302**, 419 (2003).

[4] S. Link and M. A. El-Sayed, J. Phys. Chem. B **103**, 8410 (1999).

[5] H. X. Xu, J. Aizpurua, M. Käll, and S. P. Apell, Phys. Rev. E **62**, 4318 (2000).

[6] See, e.g., A. Bouhelier, M. Beversluis, A. Hartschuh, and L. Novotny, Phys. Rev. Lett. **90**, 013903 (2003).

[7] A. J. Haes, S. L. Zou, G. C. Schatz, and R. P. Van Duyne, J. Phys. Chem. B **108**, 6961 (2004).

[8] A. J. Haes, W. P. Hall, L. Chang, W. L. Klein, and R. P. Van Duyne, Nano Lett. **4**, 1029 (2004).

[9] A. Dahlin, M. Zäch, M. Rindzevicius, M. Käll, D. Sutherland, and F. Höök, J. Am. Chem. Soc. **127**, 5043 (2005).

[10] I. Pockrand, J. D. Swalen, R. Santo, A. Brillante, and M. R. Philpott, J. Chem. Phys. **69**, 4001 (1978).

[11] A. M. Glass, P. F. Liao, J. G. Bergman, and D. H. Olson, Opt. Lett. **5**, 368 (1980).

[12] H. G. Craighead and A. M. Glass, Opt. Lett. **6**, 248 (1981).

[13] D. S. Wang and M. Kerker, Phys. Rev. B **25**, 2433 (1982).

[14] Z. Kotler and A. Nitzan, J. Phys. Chem. **86**, 2011 (1982).

[15] J. Bellessa, C. Bonnand, J. C. Plenet, and J. Mugnier, Phys. Rev. Lett. **93**, 036404 (2004).

[16] G. P. Wiederrecht, G. A. Wurtz, and J. Hranisavljevic, Nano Lett. **4**, 2121 (2004).

[17] J. Dintinger, S. Klein, F. Bustos, W. L. Barnes, and T. W. Ebbesen, Phys. Rev. B **71**, 035424 (2005).

[18] M. Moskovits, Rev. Mod. Phys. **57**, 783 (1985).

[19] T. Itoh, K. Hashimoto, A. Ikehata, and Y. Ozaki, Appl. Phys. Lett. **83**, 5557 (2003).

[20] H. X. Xu, X. H. Wang, M. P. Persson, H. Q. Xu, M. Käll, and P. Johansson, Phys. Rev. Lett. **93**, 243002 (2004).

[21] G. S. Agarwal, J. Mod. Opt. **45**, 449 (1998).

[22] A. Armitage, M. S. Skolnick, A. V. Kavokin, D. M. Whittaker, V. N. Astratov, G. A. Gehring, and J. S. Roberts, Phys. Rev. B **58**, 15367 (1998).

[23] T. Ambjörnsson and G. Mukhopadhyay, J. Phys. A **36**, 10651 (2003).

[24] T. Ambjörnsson, S. P. Apell, and G. Mukhopadhyay, Phys. Rev. E **69**, 031914 (2004).

[25] A. Ronveaux, *Heun's Differential Equations* (Oxford University Press, Oxford, 1995).

[26] S. Y. Slavyanov and W. Lay, *Special Functions: A Unified Theory based on Singularities* (Oxford University Press, Oxford, 2000), Chap. 3.

[27] L. D. Landau, E. M. Lifshitz, and L. P. Pitaevskii, *Electrodynamics of Continuous Media*, 2nd ed. (Butterworths-Heinemann, Oxford, 1984).

[28] A. A. Lucas, L. Henrard, and Ph. Lambin, Phys. Rev. B **49**, 2888 (1994).

[29] C. F. Bohren and D. R. Huffman, *Absorption and Scattering of Light by Small Particles* (Wiley, New York, 1983).

[30] A. Bagchi, R. G. Barrera, and R. Fuchs, Phys. Rev. B **25**, 7086 (1982).

[31] T. Ambjörnsson and S. P. Apell, J. Chem. Phys. **114**, 3365 (2001).

[32] A. B. Pippard, *The Physics of Vibration*, (Cambridge University Press, Cambridge, England, 1983), Vol. 2, Chap. 16.

[33] For the case of a coated cylinder ($s=1$ and $a_x \to \infty$) one could use the results for the polarizability given in Refs. 23 or 34 in order to derive a corresponding expression.

[34] L. Henrard and Ph. Lambin, J. Phys. B **29**, 5127 (1996).

[35] Some images of the local fields in and around metal ellipsoids are shown in J. P. Kottman, O. J. F. Martin, D. R. Smith, and S. Schultz, New J. Phys. **2**, 271 (2000).